ELSEVIER

Journal of Hydrology 272 (2003) 79–94

Journal of Hydrology

www.elsevier.com/locate/jhydrol

Influence of porous medium and NAPL distribution heterogeneities on partitioning inter-well tracer tests: a laboratory investigation

Marc Jalbert[†], Jacob H. Dane[*], Laurent Bahaminyakamwe

Department of Agronomy and Soils, Auburn University, Auburn, AL 36849-5412, USA

Abstract

The inter-well partitioning tracer test seemingly provides an attractive way of investigating the presence of non-aqueous phase liquids (NAPLs) in aquifers. Although the feasibility of this rather new technique has been tested in the field, only few laboratory experiments have been performed to test its validity at scales greater than the column scale. In this study, a partitioning tracer test was conducted in a nominally two-dimensional, intermediate-scale flow cell containing a tetrachloroethene (PCE) spill. Tracer breakthrough curves were obtained at 14 sampling ports and an extraction well containing three outlets. Estimated PCE contents resulting from the tracer technique were compared to PCE saturations obtained at 800 locations by gamma radiation. An inverse procedure, based on the two-site, non-equilibrium convection–dispersion equation, was used in addition to the moment method for sampling port data analysis. Although the inverse procedure produced slightly better results than the moment method, the tracer technique generally underestimated the amount of DNAPL contained in our aquifer model. Notably, our results showed that the pooled part of the DNAPL spill was not detected. This was attributed to the low aqueous phase permeability within the DNAPL pool in combination with rate-limited partitioning of the tracers into the DNAPL. Our analysis indicate a general difficulty for the tracer technique to detect NAPL located in pools or large lenses.

Keywords: Remediation; Porous media; Tetrachloroethene; PCE; DNAPL; Alcohol; Breakthrough curves; Non-equilibrium; Pools; Gamma radiation

1. Introduction

The partitioning tracer method was first extensively used in the petroleum industry (Cooke, 1971; Tang, 1992), but has recently gained interest among environmental engineers and scientists (Jackson and Pickens, 1994; Jin et al., 1995; James et al., 1997; Annable et al., 1998). The method is intended to estimate amounts of a non-aqueous phase liquids (NAPLs) present in aquifers. The technique involves the use of a partitioning and a non-partitioning tracer which are simultaneously injected into an aquifer by means of an injection well. The partitioning tracer is soluble in the NAPL present in the aquifer as well as in the carrier solution, whereas the non-partitioning tracer is soluble only in the ambient ground water. Although Wise et al. (1999) demonstrated that partitioning isotherms for commonly used tracers are non-linear, it is customary, at low tracer concentration, to consider a linear relationship between non-aqueous (c_n) and aqueous phase tracer

* Corresponding author. Tel.: +1-334-844-3974; fax: +1-334-844-3945.

E-mail addresses: danejac@auburn.edu (J.H. Dane), lbahamin@acesag.auburn.edu (L. Bahaminyakamwe).

† Deceased.

0022-1694/03/$ - see front matter © 2002 Elsevier Science B.V. All rights reserved.
PII: S0022-1694(02)00256-1

Nomenclature

a	porous medium dispersivity (L)
c	concentration of the non-partitioning tracer ($M L^{-3}$)
c_a	concentration of the partitioning tracer in aqueous phase ($M L^{-3}$)
c_n	concentration of the partitioning tracer in non-aqueous phase ($M L^{-3}$)
c_{n1}	mass of partitioning tracer in NAPL associated with instantaneous absorption divided by NAPL volume at the representative elemental volume scale ($M L^{-3}$)
c_{n2}	mass of partitioning tracer in NAPL associated with rate-limited absorption divided by NAPL volume at the representative elemental volume scale ($M L^{-3}$)
c_t	total concentration of the partitioning tracer, i.e. mass of tracer per pore volume ($M L^{-3}$)
c_0	tracer concentration of input solution ($M L^{-3}$)
C_1	non-dimensional tracer concentration of aqueous solution (–)
C_2	non-dimensional tracer concentration in NAPL associated with rate-limited absorption (–)
D	dispersion coefficient ($L^2 T^{-1}$)
F	fraction of NAPL instantaneously interacting with the partitioning tracer (–)
K	partitioning coefficient of tracer between NAPL and water (–)
L	distance between the tracer injection location and the location where the breakthrough curve is obtained (L)
P	Péclet number (–)
R	retardation factor (–)
R_F	retardation factor corresponding to the instantaneously interacting NAPL (–)
S_n	saturation of non-aqueous phase, i.e. volumetric non-aqueous phase content divided by the porosity of the porous medium (–)
t	time (T)
t_{np}	breakthrough time for non-partitioning tracer (T)
t_p	breakthrough time for partitioning tracer (T)
t_0	duration of finite pulse input (T)
T	non-dimensional time variable (–)
v	pore water velocity ($L T^{-1}$)
x	distance from input location (L)
X	non-dimensional space variable (–)
α	tracer mass transfer rate between NAPL and aqueous phase (T^{-1})
β	ratio of retardation factors corresponding to instantaneously interacting NAPL and to the total NAPL (–)
ε_2	equilibrium condition indicator (–) (Valocchi, 1985)
ω	Damkohler number (–)

concentration (c_a) at equilibrium, i.e.

$$\frac{c_n}{c_a} = K \tag{1}$$

(the notation list explains all symbols and gives their dimensions). When a partitioning and a non-partitioning tracer are injected into an aquifer simultaneously, the non-partitioning tracer molecules move with the ground water without interacting with the NAPL, while the partitioning tracer molecules move back and forth between the aqueous and non-aqueous phase (Jin et al., 1995). Consequently, the partitioning tracer transport is delayed compared to that of the non-partitioning tracer. The ratio of the partitioning tracer arrival time (t_p) and the non-partitioning tracer arrival time (t_{np}) at an extraction or observation well may be referred to as the retardation factor R. Assuming Eq. (1) to be valid at all times and locations in the porous medium (local equilibrium assumption, see Valocchi (1985)), the retardation factor can be related to the average NAPL saturation (Jin et al., 1995). Although the reader is referred to Jin et al. (1995) for a mathematical development of the relationship between R and NAPL saturation, it can also be derived upon from a probabilistic point of view. If a partitioning tracer molecule has

a probability of $1/R$ to be in the aqueous phase at a given location at any given time, then the partitioning tracer will take R times as long as the non-partitioning tracer to travel a given distance (Jury and Roth, 1990). Therefore, the retardation factor is the ratio of the total mass of partitioning tracer per pore volume and the mass of the partitioning tracer in the aqueous phase, also per pore volume (the non-aqueous phase is not moving). Hence,

$$R = \frac{t_p}{t_{np}} = \frac{c_t}{(1-S_n)c_a} = \frac{(1-S_n)c_a + S_n c_n}{(1-S_n)c_a}$$

$$= 1 + K\frac{S_n}{1-S_n} \tag{2}$$

which leads to

$$S_n = \frac{R-1}{R-1+K} \tag{3}$$

Traditionally, R is estimated by direct calculation of partitioning and non-partitioning tracer arrival times. The moment method is typically used to obtain these arrival times from breakthrough curves in response to a pulse input as stated, e.g. for the partitioning tracer by:

$$t_p(x) = \frac{\int_0^\infty t c_a(x,t)\mathrm{d}t}{\int_0^\infty c_a(x,t)\mathrm{d}t} \tag{4}$$

In the above expression the breakthrough time corresponds to the time at which half of the tracer mass has arrived at the observation location. For a step input with the concentration of the aqueous tracer changing from c_0 to 0, the arrival time is equated to the normalized surface under the breakthrough curve:

$$t_p(x) = \int_0^\infty \frac{c_a(x,t)}{c_0}\mathrm{d}t \tag{5}$$

For a step input with the aqueous tracer concentration changing from 0 to c_0, the arrival time is

$$t_p(x) = \int_0^\infty \frac{c_0 - c_a(x,t)}{c_0}\mathrm{d}t \tag{6}$$

The expressions stated so far are based on the local equilibrium assumption. However, it can be shown (Harvey and Gorelick, 1995) that Eq. (2) is theoretically still valid under non-equilibrium conditions and for a non-uniform NAPL distribution. In that case, Eq. (2) gives the average retardation factor along the streamline passing through a sampling point (port) or for that region of the aquifer associated with the aqueous phase that is intercepted by an extraction well. Therefore, the partitioning tracer technique can theoretically be carried out without knowledge of the NAPL and/or the partitioning tracer exchange rate distribution. In this paper, we investigated the validity of this assertion by studying the cumulated influence of non-equilibrium conditions and NAPL non-uniformity on a partitioning tracer test performed in an intermediate-scale flow cell.

A repercussion of non-equilibrium tracer partitioning on breakthrough curves is the so-called tailing, i.e. in response to a pulse input, the breakthrough curve of the partitioning tracer shows a long-lasting decrease in tracer concentration. Other factors contributing to tailing are non-uniform NAPL distributions, permeability contrasts, and dilution effects. Especially the presence of NAPL pools or lenses, where greatly reduced aqueous phase permeabilities exist, would seem to contribute to long-term tailing. Tailing creates uncertainty in the numerical integration of the curve or, in case of missing tail data, results in an underestimation of the arrival time. To overcome this drawback when applying the moment method, Annable et al. (1998) extrapolated missing tail data assuming empirical exponential decay. In an attempt to limit tailing-induced errors in the estimation of retardation factors, and to determine to what extent our partitioning tracer test was under the influence of non-equilibrium partition, we analyzed breakthrough curves with a fitting procedure taking into account the kinetics of tracer transfer between the aqueous and non-aqueous phase. We made use of the non-dimensional form of the one-dimensional, non-equilibrium convection–dispersion equation (CDE) for modeling transport of the partitioning tracer, as suggested by Hatfield et al. (1993). The method was easily implemented since analytical solutions for the non-dimensional CDE and curve fitting procedures are readily available (Parker and van Genuchten, 1984; Toride et al., 1995). The results of this technique and the moment method were compared to actual saturation values determined by gamma radiation scanning.

1.1. Non-equilibrium inverse procedure

Following a NAPL spill into an aquifer, the NAPL is likely to exist in different forms. It will not only exist in residual form, but also as ganglia, lenses, and pools of different sizes. These different forms will have different exchange properties with respect to tracers present in the aqueous phase. In an attempt to incorporate the influence of different NAPL occurrences in our aquifer model, we considered a two-site partitioning model as the basis of an inverse analysis of partitioning tracer breakthrough curves (Brusseau, 1992; Hatfield et al., 1993; Nkeddi-Kizza et al., 1984; Cussler, 1984; van Genuchten and Wagenet, 1989; Sardin et al., 1991). Analogous to the earlier developed two-site model (Selim et al., 1976) for solid–liquid interactions, we assumed a fraction F of the NAPL to consist of instantaneous sites, where equilibrium conditions exist, and a fraction $(1-F)$ of rate-limited sites, for which first-order mass transfer between aqueous and non-aqueous phase was adopted. The basic premise of this approach is to capture partitioning tracer exchange phenomena for which no mathematical descriptions are yet available, especially those related to heterogeneities (Nelson et al., 1999). Considering no adsorption on solid particles, the one-dimensional convection–dispersion equation, describing transport of a tracer partitioning into residual NAPL at saturation S_n, can then be expressed as

$$(1-S_n)\frac{\partial c_a}{\partial t}+S_n\frac{\partial c_{n1}}{\partial t}+S_n\frac{\partial c_{n2}}{\partial t} = (1-S_n)D\frac{\partial^2 c_a}{\partial x^2}-(1-S_n)v\frac{\partial c_a}{\partial x} \tag{7a}$$

$$c_{n1}=FKc_a \tag{7b}$$

$$\frac{\partial c_{n2}}{\partial t}=\alpha[(1-F)Kc_a-c_{n2}] \tag{7c}$$

These equations were obtained following the argument presented by van Genuchten and Wagenet (1989) for describing two-site adsorption on solid surfaces. Eqs. (7a)–(7c) are similar to submodel 3 of Hatfield et al. (1993), except that we make use of NAPL saturation and a liquid–liquid partitioning coefficient (K), while these authors chose to formulate their model in terms consistent with adsorption on solid surfaces. We would like to point out that the above model does not include any description of exchange between potential zones of immobile water and bulk ground water flow. It was assumed that the influence of immobile water on tracer transport was limited, and that it could be incorporated in the value of the dispersion coefficient D, following the approach of Passioura (1971).

Using the following non-dimensional variables

$$T=\frac{vt}{L} \tag{8a}$$

$$X=\frac{x}{L} \tag{8b}$$

$$P=\frac{vL}{D} \tag{8c}$$

$$C_1=\frac{c_a}{c_0} \tag{9a}$$

$$C_2=\frac{c_{n2}}{(1-F)Kc_0} \tag{9b}$$

$$R=1+\frac{KS_n}{(1-S_n)} \tag{10a}$$

$$R_F=1+\frac{FKS_n}{(1-S_n)} \tag{10b}$$

$$\beta=\frac{R_F}{R} \tag{11a}$$

$$\omega=\frac{\alpha(1-\beta)RL}{v} \tag{11b}$$

the transport equations take the form:

$$\beta R\frac{\partial C_1}{\partial T}+(1-\beta)R\frac{\partial C_2}{\partial T}=\frac{1}{P}\frac{\partial^2 C_1}{\partial X^2}-\frac{\partial C_1}{\partial X} \tag{12a}$$

$$(1-\beta)R\frac{\partial C_2}{\partial T}=\omega(C_1-C_2) \tag{12b}$$

The convection–dispersion equation for the partitioning tracer is thus available in the non-dimensional, classical form used for physical and chemical non-equilibrium (Nkeddi-Kizza et al., 1984; Leij and Toride, 1998). The model used herein (special case of model 4 of Brusseau (1992); submodel 3 of Hatfield et al. (1993)) is thus equivalent to the two-site adsorption model first proposed by Selim et al. (1976) and Cameron and Klute (1977) and to the model describing solute transport in sorptive and aggregated porous media presented by van Genuchten

and Wierenga (1976). The reader should notice that when no instantaneous sites are considered ($F = 0$, $R\beta = 1$), the form of the model we used further reduces to the non-equilibrium adsorption model of Lapidus and Amundson (1952) and to the mobile–immobile water model of Coats and Smith (1964). The choice of a two-site model is supported by experimental work of Augustijn et al. (1991) and Hatfield et al. (1993), who demonstrated that Eqs. (12a) and (12b) can successfully describe transport of partitioning tracers in sand columns containing a rather uniform residual NAPL. The two-site model was subsequently implemented in a fully inverse fitting procedure to estimate parameters such as NAPL amounts and transfer rates between the aqueous and organic phase. Even though the NAPL saturation was not uniform during our experiments, it was believed that an inverse procedure using Eqs. (12a) and (12b) would be successful in estimating meaningful retardation factors. Support to our approach was presented by Leij and Dane (1991), who concluded that tracer retardation depends only on the amount of absorption and not on the absorption distribution. The procedure, which only uses partitioning and non-partitioning tracer breakthrough curve information, was thus tested as an alternative to the classical moment method. Five parameters, other than L and c_0, are needed to model the partitioning tracer transport according to Eqs. (12a) and (12b): v, D, R, β, and ω. Because the non-partitioning tracer is unaffected by the presence of the NAPL, its transport can be used to independently obtain values for the pore water velocity and the dispersion coefficient, which are physical properties that also apply to the partitioning tracer transport. Consequently, we fitted the non-partitioning tracer breakthrough curves to solutions of the conventional CDE

$$\frac{\partial c}{\partial t} = D\frac{\partial^2 c}{\partial x^2} - v\frac{\partial c}{\partial x} \tag{13}$$

Because dispersion coefficient and aqueous phase velocity are physically related by the notion of dispersivity (Bear, 1972), we checked the mathematical uniqueness of the sets of values obtained through breakthrough curve fitting. This was done by verifying that the set of parameters returned by the optimization scheme was insensitive to the values of the initial parameter guesses. Once values for v and D were obtained from the non-partitioning tracer breakthrough curve, they were used as fixed parameters during fitting of the partitioning tracer breakthrough curve with solutions of Eqs. (12a) and (12b). This last step resulted in estimates for the parameters R, β, and ω. Estimates for average NAPL contents were then calculated from Eq. (3), and the proportion of instantaneous sites F was obtained from Eqs. (10a), (10b) and (11a) as

$$F = \frac{R\beta - 1}{R - 1} \tag{14}$$

The inverse technique was easily implemented by making use of the CXTFIT2 program (Parker and van Genuchten, 1984; Toride et al., 1995), which incorporates analytical solutions of Eqs. (12a), (12b) and (13), and also contains a Levenberg–Marquardt optimization algorithm.

2. Materials and methods

Non-partitioning and partitioning tracer breakthrough curves were obtained at 14 extraction ports and three outlets inside an extraction well in a nominally two-dimensional flow cell containing a 1-liter tetrachloroethene (PCE) spill. The rectangular porous medium (167 cm long, 62 cm high, 5 cm wide) consisted of coarse sand (F4.0 Flintshot Ottawa Sand; F&S Abrasives, Birmingham, AL) with embedded lenses of finer sands (Table 1; F2.8 and F75). The sands were packed under water. The porous medium configuration and the locations of sampling ports (solid circles) and wells are presented in Fig. 1, while a complete description of the flow cell is given by Oostrom et al. (1999). The horizontally dashed line at an elevation of about 35 cm represents a kaolinite layer of about 3-cm thickness. It was applied as a paste to prevent PCE from moving to the bottom of the flow cell and out of reach of the gamma radiation system to determine S_n.

2.1. Spill behavior

One liter of tetrachloroethene (PCE) was spilled into the water-saturated porous medium by maintaining a pressure slightly exceeding the displacement pressure in a constant head device. The surface of

Table 1
Porous medium properties

	Sand		
	F4.0	F2.8	F75
Texture	Coarse	Fine	Very fine
Particle size (% total mass)			
< 106 m	0.07	0.44	2.70
106–250 m	0.86	14.4	47.5
250–500 m	7.9	42.5	49.7
500–840 m	90.5	42.6	0.02
> 840 m	0.7	0.44	0
Porosity	0.35	0.36	0.41
Standard deviation	0.012	0.014	0.019
Bulk density (kg/m^3)	1720	1696	1564
Air–water displacement pressure (kPa)	1.3	2.1	4.6
Saturated hydraulic conductivity $\times 10^3$ (m/s)	1.3	0.36	0.11

the porous medium closely matched the level of the water table. The PCE (DNAPL) spill exhibited very little fingering and its movement occurred downwards and laterally until it reached the very fine sand (F75) lens, approximately 5 min after the beginning of the spill. Because of a higher displacement capillary pressure and a lower permeability value than for the surrounding sand (Table 1), the PCE only temporarily entered this layer and only for a few mm, but mainly spread out laterally, in a fairly symmetric way. The subsequent downward and somewhat lateral movement then took place along the two edges of the very fine sand lens. The downward flow was only slightly affected by the presence of the two lower fine sand (F2.8) lenses. They were easily invaded by the DNAPL, because they had a smaller displacement capillary pressure and a greater permeability value than the very fine sand lens above (Table 1; Fig. 1). After about 21 min the PCE reached the bottom of the coarse sand, where it was intercepted by the impermeable clay layer. It subsequently spread out and formed a pool. Gamma radiation measurements to determine PCE saturations in the flow container were obtained at different times at 800 locations (Fig. 2). It should be noted that the highest density of measurement locations existed at the elevations of the embedded sand and clay lenses. The gamma radiation method consisted of the single source (^{241}Am) procedure described by Oostrom et al. (1998) (relative probable error for NAPL saturations $\approx$1%). Fig. 3 shows the PCE saturation content distribution as measured by gamma radiation 8 d after the spill. It clearly shows how the PCE bypassed the very fine sand layer, accumulated somewhat in the two lower fine sand layers, and accumulated and spread out on top of the clay lens. Saturation values just above the clay lens were as high as 0.7. Mainly because of its very low

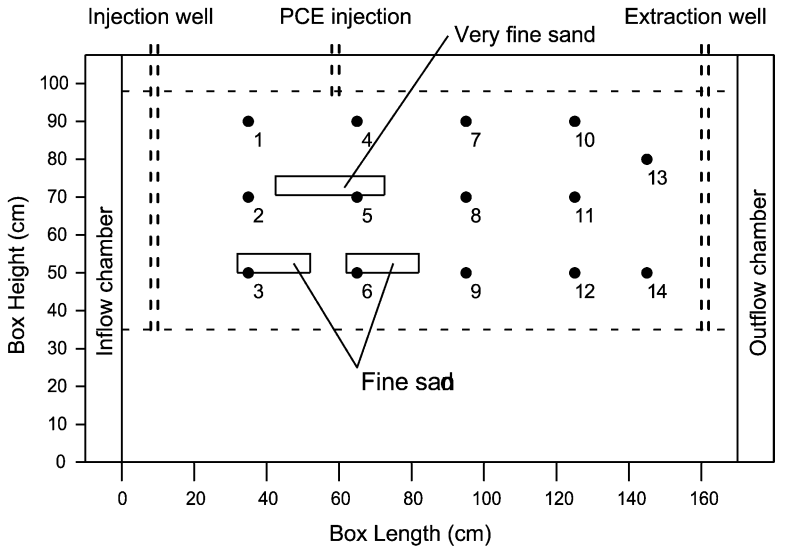

Fig. 1. Schematic of the Auburn University flow container and porous medium configuration.

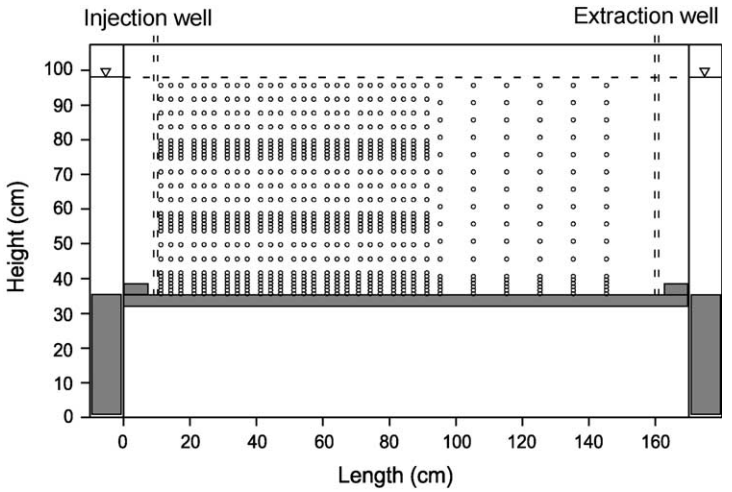

Fig. 2. Gamma radiation measurement locations.

solubility in water, no change in the PCE distribution was observed at larger times, and the data comprising Fig. 3 were used to calculate the PCE amount in the flow container.

2.2. Flow of tracers

2-Propanol ($K \approx 0$ between water and PCE; Wang et al., 1998) was used as the non-partitioning tracer, while 2,3-dimethyl-2-butanol ($K = 3.15$ between PCE and water, standard deviation: 0.05) and 1-hexanol ($K = 7.35$ between PCE and water, standard deviation: 0.16) comprised the partitioning tracers. Values for the partitioning coefficients were obtained in batch experiments (five replicates for each tracer), following the procedure of Wang et al. (1998). The composite tracer solution, at a concentration of 1000 mg/l for each tracer, was injected into the flow container through a well (inside diameter 7.2 mm, outside diameter 9.6 mm) perforated over its entire height and situated 10 cm from the left (upstream) end of the porous medium. Extraction occurred from a similar well located 10 cm from the right end of the container (Fig. 1). A flow rate of 8.6 ml/min was maintained with three Masterflex® pumps (Cole-Parmer Instrument Company), each equipped with

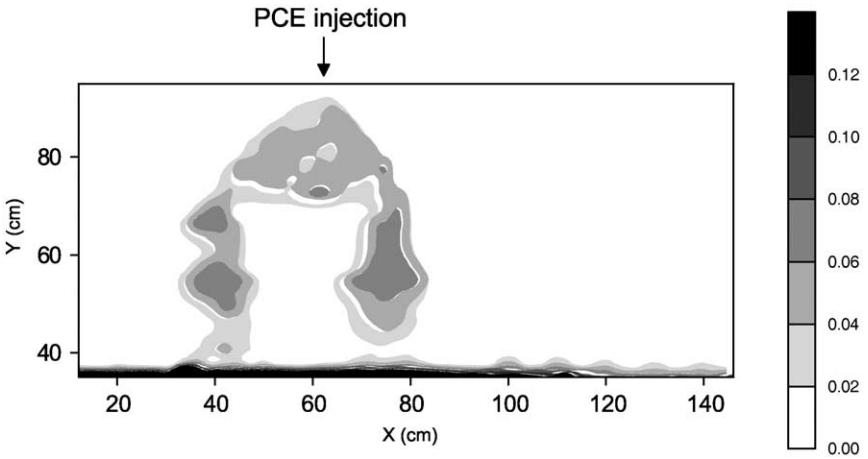

Fig. 3. PCE distribution as recorded by gamma radiation 8 d after PCE spill. Numbers indicate PCE saturations. It should be noted that saturation values near the bottom boundary of the flow domain (clay lens) were as high as 0.7.

two model 70 16–20 heads. The solution could thus be applied (injection well) and extracted (extraction well) through three tubings, respectively. The outlets and inlets of the tubings were equally spaced within the wells to provide an even distribution. The preset flow rate resulted in an inter-well residence time of 31.5 h. The composite tracer solution was dyed with fluorescein to observe the displacement of water by the tracer solution using ultraviolet lights. Knowledge of the approximate location of the displacement front helped to limit the number of samples to be collected at the 14 extraction ports (Fig. 1). It should be noted that the displacement front was very much vertical (photographically recorded but not shown here), indicating no density effect by the aqueous solutions (Dane et al., 1999). The frequency of sampling was increased when the front approached an extraction port. We found that port 10 was partially clogged, possibly because of precipitation of fluorescein dye used in prior experiments. After injection of approximately 1.5 pore volumes of tracer solution, deionized water replaced the tracer solution as the injection fluid. The respective durations of the tracer pulse (about 48 h) and of the subsequent deionized water flush (>48 h) were assumed to be sufficiently long to each constitute a step input. The advance of the non-dyed water was again recorded by photography, and about the same number of samples was obtained at the 14 extraction ports and extraction well as for the previous step change.

2.3. Chemical analysis

Concentrations of the three alcohols (2-propanol, 2,3-dimethyl-2-butanol, and 1-hexanol) were determined with a gas chromatograph (Hewlett-Packard 6890A, Hewlett Packard Co., Wilmington, DE), equipped with a standard glass capillary column (HP-5 5% phenyl methyl siloxane, 30 m × 250 μm × 250 μm), a flame ionization detector (FID), and an auto-sampler to allow continuous analysis. The carrier gas was helium. Hydrogen and air (oxygen source) were used as the burning fuel. The retention time was determined for each alcohol and, based on peak area readings, a calibration curve for each alcohol was obtained using the following concentrations: 0, 20, 40, 60, 80, 120, 200, 400, 600, 800, 1000, 1200, and 4000 mg/l. Hewlett-Packard ChemStations software was used to integrate areas under the chromatography curves. To establish breakthrough curves, 3–4 ml solution samples were extracted, placed in glass test tubes and mixed by shaking. Part of the solution was then transferred to fill 2.0 ml glass sample vials, which were closed with blue Teflon® and red rubber caps to secure an evaporation-proof seal. The exact time of extraction was recorded for all samples. All standards used in the gas chromatography calibration were run at the beginning and the end of each set of samples belonging to each port. During the chromatographic analyses, the temperature was first increased to 200 °C at a rate of 25 °C/min, where it was maintained for 1 min. It was subsequently further increased at the same rate to 300 °C, where it was kept constant for 3 min. Finally, the temperature was decreased to 40 °C and maintained for 1 min before the next run. The capillary column was cleaned each time five samples had been analyzed by increasing the oven temperature to 300 °C at a rate of 25 °C/min and maintaining it for 3 min. This study represents a total of 870 concentration determinations.

2.4. Breakthrough curve analysis

The breakthrough curves collected at the 14 sampling ports were analyzed using the program CXTFIT2 (Toride et al., 1995), which makes use of a Levenberg–Marquardt algorithm to fit analytical solutions of the equilibrium and non-equilibrium CDE to experimentally obtained breakthrough curves. The 2-propanol data were fitted using the conventional CDE option, because no retardation or tailing was supposed to occur with this tracer. Two parameters were fitted, v and D. The fitting procedure was insensitive to the initial guesses for these parameters, indicating the mathematical uniqueness of the obtained sets of values. The 2-3-DMB and 1-hexanol data were fitted using the two-site non-equilibrium adsorption model, equivalent to Eqs. (12a) and (12b). Three parameters were fitted simultaneously: R, β, and ω. The two other parameters (v and D) were fixed at the values obtained for the 2-propanol data. The CXTFIT2 Levenberg–Marquardt optimization algorithm did, however, not always result in unique values for R, β and ω. To obtain the best possible fit, different initial guesses were generated with a random number

generator and values corresponding to the highest correlation coefficients were chosen.

The breakthrough curves obtained at the extraction ports were also analyzed by the moment method using Eqs. (5) and (6). The arrival times of the different tracers were calculated by estimating the area under the breakthrough curve by numerical integration, using the trapezoidal rule. Because of the porous medium and DNAPL distribution heterogeneity, the three breakthrough curves obtained at the extraction well exhibited too much tailing for the hypothesis of having step inputs to be valid. Consequently, we considered a finite pulse input as the boundary condition for estimating the tracers' arrival times at the extraction well. The mathematical formula for calculating, e.g. the partitioning tracer breakthrough time in case of a finite pulse input, starting at time $t = 0$ and of duration t_0, is given by Jin et al. (1995):

$$t_p(x) = \frac{\int_0^\infty t c_a(x,t)\mathrm{d}t}{\int_0^\infty c_a(x,t)\mathrm{d}t} - \frac{t_0}{2} \quad (15)$$

Retardation factors were obtained as the ratios of the partitioning and non-partitioning tracers' arrival times. PCE saturations were subsequently calculated from knowledge of the retardation factors (Eq. (3)).

3. Results and discussion

3.1. Sampling port data

Because the breakthrough curves collected at the extraction well were very much influenced by the porous medium and PCE distribution heterogeneity, the one-dimensional, non-equilibrium CDE could not correctly model the obtained results, and the inverse procedure was only used on port data sets. Two non-partitioning tracer data sets and four partitioning tracer data sets were obtained for each port, because we employed a step input from 0 to 1000 mg/l (noted left) followed by a step input from 1000 to 0 mg/l (noted right). An example of the good fit between experimental data and the CXTFIT2 fitting procedure is given in Fig. 4, representing breakthrough curves for the three tracers at port 12 (Fig. 1) in response to step inputs with relative concentrations changing from 0 to 1 (left) and subsequently from 1 to 0 (right). Results of the analysis performed on the non-partitioning tracer (2-propanol) breakthrough curves are summarized in Table 2. High correlation coefficients showed the ability of the conventional CDE (Eq. (13)) to describe the flow of the non-partitioning tracer. Porous medium and PCE distribution heterogeneity are believed to be the cause of

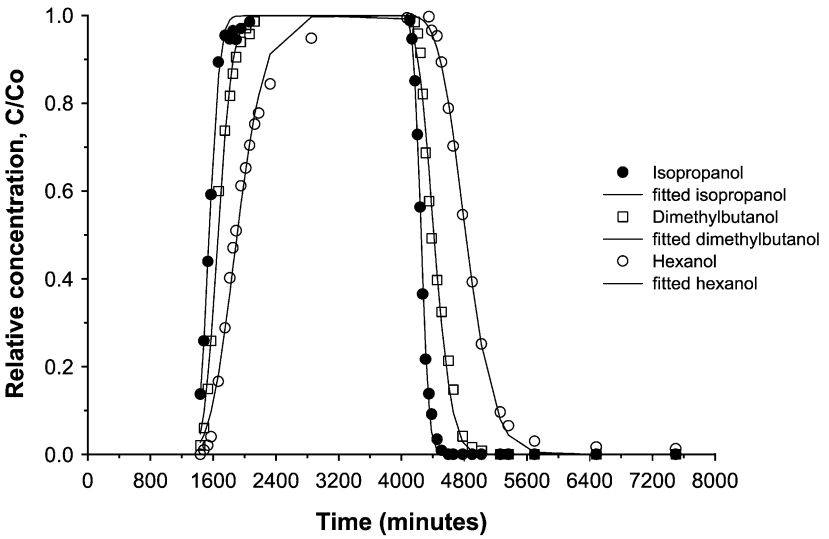

Fig. 4. Experimental breakthrough data obtained at port 12 in response to step input with the relative concentration changing from 0 to 1, and 1 to 0, respectively, and the curves fitted with CXTFIT2.

Table 2
Numerical results of the analysis of non-partitioning tracer breakthrough curves by the moment method and the conventional CDE fitting procedure. v is pore water velocity, D is diffusion/dispersion coefficient, and r^2 is correlation coefficient

Port	Step	Moment method; v (cm/min)	Inverse procedure		
			v (cm/min)	D (cm^2/min)	r^2
1	Left	0.097	0.102	0.0050	0.9982
	Right	0.112	0.082	0.0107	0.9995
2	Left	0.081	0.084	0.0118	0.9994
	Right	0.110	0.080	0.0097	0.9994
3	Left	0.079	0.074	0.0141	0.9920
	Right	0.111	0.081	0.0081	0.9997
4	Left	0.095	0.096	0.0072	0.9990
	Right	0.096	0.084	0.0109	0.9986
5[a]	Left	0.083	0.085	0.0189	0.9813
	Right	0.084	0.081	0.0229	0.9757
6	Left	0.077	0.077	0.0064	0.9959
	Right	0.098	0.086	0.0133	0.9987
7	Left	0.090	0.091	0.0056	0.9993
	Right	0.081	0.078	0.0226	0.9936
8	Left	0.080	0.081	0.0093	0.9994
	Right	0.082	0.077	0.0054	0.9991
9	Left	0.080	0.081	0.0173	0.9923
	Right	0.095	0.087	0.0137	0.9990
10[b]	Left	0.084	0.085	0.0044	0.9975
	Right	0.067	0.067	0.0084	0.9752
11[a]	Left	0.073	0.074	0.0095	0.9986
	Right	0.064	0.068	0.0841	0.9296
12	Left	0.074	0.074	0.0193	0.9927
	Right	0.086	0.081	0.0146	0.9985
13[c]	Left	0.078	0.081	0.0113	0.9781
	Right	0.077	0.073	0.0048	0.9997
14	Left	0.070	0.070	0.091	0.9971
	Right	0.081	0.077	0.0116	0.9980

[a] Flow and transport affected by the presence of the very fine sand layer.
[b] Port affected by fluorescein dye precipitation.
[c] Limited number of recorded data for the first step at this port.

deviations between CDE solutions and experimental breakthrough curves for ports 5 and 11, which showed tailing due to the slow tracer release from the very fine sand lens. Results for port 10 were influenced by partial clogging (see Section 2). Generally speaking, the moment method and the conventional CDE inverse procedure resulted in similar estimations of the tracer arrival times, and consequently in similar estimations of the mean aqueous phase velocity (moment method: $v_{\text{average}} = 0.085$, S.D. $= 0.013$; inverse procedure: $v_{\text{average}} = 0.081$, S.D. $= 0.008$). For a majority of the breakthrough data sets, it seemed, therefore, justified to use the v- and D-values determined with the non-partitioning tracer for further analysis of the partitioning tracer data, using inverse modeling applied to Eqs. (12a) and (12b). Table 3 contains the results of the different analysis performed on partitioning tracer breakthrough curves, together with PCE saturation (S_n) estimates obtained by gamma radiation scanning (diameter of collimated gamma radiation beam equals 6 mm; beam length equals thickness of flow cell). The listed S_n values were obtained by averaging the measured values along the horizontal line upstream from each sampling port by trapezoidal integration to allow proper comparison with the average PCE values obtained with the moment and inverse methods. We thus assumed, based on photographic evidence, that the streamlines between injection and extraction wells were essentially horizontal. High correlation coefficients show that the partitioning tracers' breakthrough curves were accurately fitted by solutions of the two-site non-equilibrium CDE. However, quantitative discrepancies were found between estimated PCE saturations obtained by the inverse procedure and gamma radiation, which may have been the result of the model not truly representing the physical conditions during the experiment. The moment method analysis (Table 3) did not result in better DNAPL content estimations. To estimate the accuracy of each method, we calculated the average relative deviation between the data obtained with the tracer methods and the gamma radiation results, which were assumed to represent our reference values, as

$$\left\langle \frac{\Delta S_n}{S_n} \right\rangle = \left\langle \frac{|S_n^i - S_n^{\text{gamma}}|}{S_n^{\text{gamma}}} \right\rangle \tag{16}$$

where i indicates either the moment method or the CDE-based inverse procedure. Ignoring the data obtained at port 1, the inverse procedure ($\langle \Delta S_n/S_n \rangle = 0.28$) was found to produce somewhat better estimates of PCE saturations than the moment method ($\langle S_n/S_n \rangle = 0.37$). Figs. 5 and 6 show that both methods generally resulted in an underestimation of the PCE amounts contained in our aquifer model. In some cases, however, the moment method resulted in large relative overestimations of PCE saturation. These

Table 3
Numerical results of the analysis of partitioning tracers breakthrough curves by the moment method and the non-equilibrium CDE inverse procedure, as compared to saturation estimates obtained by gamma radiation scanning. S_n is PCE saturation, F is proportion of instantaneous absorption sites, ω is the Damkohler number, and r^2 is correlation coefficient

Port	Tracer	Step	Gamma radiation S_n	Moment method S_n	Two-site non-equilibrium CDE inverse procedure S_n	F [a]	ω	r^2
1	2-3-DMB	Left	0.000	0.011	0.003	−0.08	0.003	0.9990
		Right	0.000	0.010	0.012	−0.10	0.003	0.9998
	1-Hexanol	Left	0.000	0.007	0.006	0.04	0.011	0.9984
		Right	0.000	0.053	0.027	0.08	0.004	0.9994
2	2-3-DMB	Left	0.049	0.018	0.035	0.14	0.043	0.9997
		Right	0.049	0.048	0.035	0.44	0.019	0.9998
	1-Hexanol	Left	0.049	0.043	0.050	0.19	0.067	0.9989
		Right	0.049	0.095	0.050	0.31	0.061	0.9984
3	2-3-DMB	Left	0.057	0.070	0.060	0.48	0.004	0.9965
		Right	0.057	0.053	0.040	0.22	0.031	0.9998
	1-Hexanol	Left	0.057	0.068	0.057	0.43	0.019	0.9986
		Right	0.057	0.103	0.051	0.11	0.145	0.9975
4	2-3-DMB	Left	0.051	0.048	0.048	−0.15	0.113	0.9942
		Right	0.051	0.049	0.045	0.66	0.013	0.9999
	1-Hexanol	Left	0.051	0.061	0.060	0.37	0.043	0.9996
		Right	0.051	0.070	0.056	0.79	0.009	0.9921
5[b]	2-3-DMB	Left	0.076	0.042	0.055	0.50	0.005	0.9984
		Right	0.076	0.044	0.070	0.46	0.004	0.9973
	1-Hexanol	Left	0.076	0.061	0.064	0.49	0.016	0.9995
		Right	0.076	0.062	0.065	0.66	0.005	0.9982
6	2-3-DMB	Left	0.095	0.039	0.043	0.45	0.008	0.9989
		Right	0.095	0.059	0.057	0.35	0.023	0.9999
	1-Hexanol	Left	0.095	0.054	0.055	0.28	0.028	0.9990
		Right	0.095	0.092	0.075	0.55	0.030	0.9989
7	2-3-DMB	Left	0.048	0.024	0.027	0.68	0.004	0.9996
		Right	0.048	0.031	0.040	0.69	0.001	0.9968
	1-Hexanol	Left	0.048	0.041	0.039	0.44	0.024	0.9991
		Right	0.048	0.041	0.045	0.79	0.001	0.9941
8	2-3-DMB	Left	0.071	0.056	0.057	0.38	0.040	0.9988
		Right	0.071	0.044	0.051	0.51	0.024	0.9998
	1-Hexanol	Left	0.071	0.079	0.079	0.38	0.043	0.9995
		Right	0.071	0.060	0.061	0.77	0.013	0.9989
9	2-3-DMB	Left	0.102	0.044	0.049	0.54	0.006	0.9993
		Right	0.102	0.055	0.052	0.38	0.011	0.9952
	1-Hexanol	Left	0.102	0.061	0.062	0.37	0.019	0.9994
		Right	0.102	0.084	0.073	0.43	0.050	0.9990
10[c]	2-3-DMB	Left	0.041	0.014	0.018	0.55	0.006	0.9977
		Right	0.041	0.017	0.041	−0.11	0.008	0.9994
	1-Hexanol	Left	0.041	0.025	0.025	0.52	0.010	0.9884
		Right	0.041	0.022	0.027	0.42	0.005	0.9976
11[b]	2-3-DMB	Left	0.059	0.026	0.031	0.54	0.001	0.9984
		Right	0.059	0.034	0.069	0.03	0.006	0.9988
	1-Hexanol	Left	0.059	0.046	0.049	0.27	0.024	0.9983
		Right	0.059	0.037	0.055	0.74	0.001	0.9885
12	2-3-DMB	Left	0.083	0.023	0.025	0.55	0.004	0.9969
		Right	0.083	0.042	0.041	0.21	0.010	0.9974
	1-Hexanol	Left	0.083	0.036	0.036	0.39	0.010	0.9994

(*continued on next page*)

Table 3 (*continued*)

Port	Tracer	Step	Gamma radiation S_n	Moment method S_n	Two-site non-equilibrium CDE inverse procedure S_n	F [a]	ω	r^2
		Right	0.083	0.061	0.055	0.33	0.035	0.9994
13	2-3-DMB	Left	0.047	0.024	0.034	0.82	0.001	0.9985
		Right	0.047	0.025	0.023	0.73	0.004	0.9998
	1-Hexanol	Left	0.047	0.040	0.043	0.52	0.019	0.9995
		Right	0.047	0.034	0.030	0.70	0.014	0.9982
14	2-3-DMB	Left	0.074	0.019	0.019	0.49	0.003	0.9991
		Right	0.074	0.037	0.038	0.10	0.008	0.9933
	1-Hexanol	Left	0.074	0.027	0.026	0.39	0.011	0.9997
		Right	0.074	0.055	0.050	0.20	0.030	0.9996

[a] Negative values for F, as resulting from the optimization process performed on our data, are due to experimental uncertainties and should be thought of as zero.
[b] Flow and transport affected by the presence of the very fine sand layer.
[c] Port affected by fluorescein dye precipitation.

overestimations occurred at ports located near the injection well, where experimental uncertainties were high, because partitioning and non-partitioning tracers had had little opportunity to separate, and the gamma radiation estimates at these locations were calculated from few measurement locations. Consequently, these overestimations might represent experimental uncertainties more than a fallacy of the moment method. Overall the tracer technique applied at the sampling ports did not produce perfect estimations of PCE saturations, but was a fairly good indicator of the amounts of residual contaminant.

The values given by the inverse procedure for the fraction of instantaneous equilibrium sites F (Table 3) showed a great deal of variability ($F_{average} = 0.4$; S.D. = 0.24). These findings are rather difficult to interpret, since even values obtained at the same port are often quite different. This might indicate,

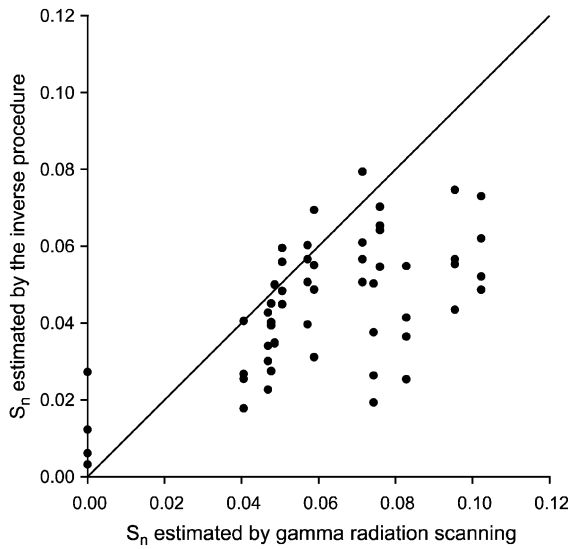

Fig. 5. Comparison of average PCE saturation (S_n) data determined with the inverse procedure based on CXTFIT2 (sampling port data) and gamma radiation estimates. The solid line represents to 1:1 ratio.

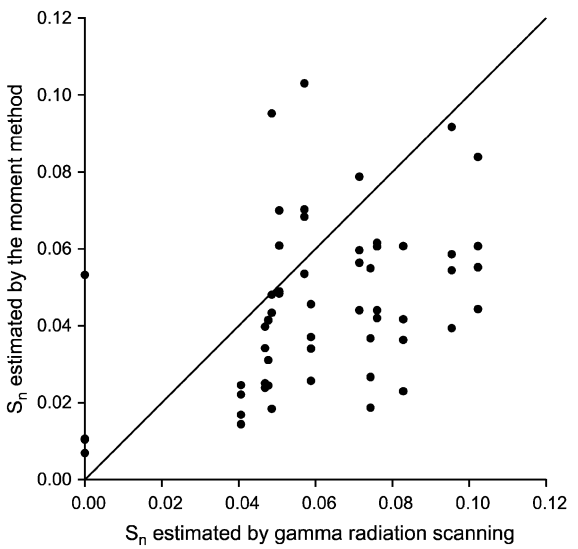

Fig. 6. Comparison of average PCE saturation (S_n) data determined with the moment method (sampling port data) and gamma radiation estimates. The solid line represents to 1:1 ratio.

however, a variability in the PCE occurrences in our aquifer model. Large DNAPL lenses should be more prone to rate-limited conditions than small ganglia or films, because of their smaller surface to volume ratio. Some negative values for F were obtained, which, again, were attributed to the uncertainties in the experimental data obtained at the extraction ports located near the injection well and port 10.

The values obtained for the Damkohler number ω (Brusseau, 1992) (Table 3) should also be interpreted with caution, because in the two-site CDE model they apply to the non-equilibrium sites only. The PCE zones that were interpreted by the CDE model as instantaneous sites were probably exhibiting ω-values orders of magnitude greater than the values reported in Table 3. Average values for R_F were 1.12 (S.D. = 0.088) and 1.17 (S.D. = 0.105) for 2,3-dimethyl-2-butanol and 1-hexanol, respectively, while those for R were 1.31 (S.D. = 0.131) and 1.38 (S.D. = 0.138), respectively.

3.2. Well outlet data

The breakthrough curves obtained at the extraction well were analyzed by the moment method (Eq. (15)). Estimated DNAPL saturations were obtained from the arrival times of the tracers, by using Eqs. (2) and (3). These saturations were then averaged, since each outlet was supposed to represent one-third of the flow domain. The saturation estimates were multiplied by the pore volume between injection and extraction well, leading to estimates for the total amount of PCE contained in the flow cell. The method using 2,3-dimethyl-2-butanol as the partitioning tracer estimated a total of 380 ml PCE, while the 1-hexanol curves resulted in an estimate of 499 ml. Consequently, the two tracers severely underestimated the volume of PCE contained in the flow cell, which was 1000 ml. This underestimation was also observed for the sampling port data, most of which were thought to relate to PCE present in residual form. The pool at the bottom of the flow cell represented approximately 30% of the total PCE present in the container (calculated by trapezoidal, two-dimensional integration of the gamma radiation data; total PCE volume estimated by the integration: 0.99 l). To assess how much of the DNAPL pool was detected by the partitioning tracer test, we assumed that the underestimation of residual PCE for the well outlet data was approximately the same as the underestimation observed at the sampling ports. If 30% of the residual DNAPL was not detected, based on the average for all sampling port data, then the observed inter-well estimations of the PCE amount contained in our aquifer model are only reasonable if the pooled part of the spill had no influence on the test ($0.7 \times 0.7\,\text{l} \approx 0.5\,\text{l}$ as obtained for the best data set, viz. 1-hexanol data). These coarse estimates tend to suggest that the inter-well partitioning tracer test could not detect any PCE from the pool located at the bottom of our two-dimensional aquifer model.

3.3. Interpretation

To summarize our findings, the partitioning tracer test performed on a PCE spill contained in a two-dimensional aquifer model resulted in considerable underestimations of the spilled DNAPL. The well outlet data suggest that the tracer technique was blind to the pooled part of the spill, which is typically a zone of high DNAPL contents with a slow transfer of tracer between the aqueous and non-aqueous phase liquid. This slow exchange of a partitioning tracer in high DNAPL content zones is due to the low surface to volume ratio of the contaminant and the diminished permeability to water in zones surrounding the pollutant (water occupies the smaller pores). These zones of low permeability to water impede the partitioning tracer exchange by acting as a buffer between the DNAPL and the region of bulk ground water flow (Brusseau, 1992; Hatfield et al., 1993). During a tracer test, the amount of partitioning tracer that has time to move into high DNAPL content zones is low compared to the total mass of tracer injected. The subsequent release of these partitioning tracer molecules from DNAPL pools or large lenses is also slow. Consequently, the contribution of slow transfer zones to partitioning tracer breakthrough curves collected downstream from a spill is a long lasting arrival of tracer at low concentration. When using a well or a vertically integrated port for tracer extraction, this low concentration is even further diluted. NAPL pools and large lenses remain, therefore, largely undetected by the partitioning tracer test. Unfortunately,

these NAPL occurrences may represent large proportions of the total NAPL mass present in the aquifer, or may even be the only source of contamination when the residual pollutant has completely dissolved into the ground water, as is often the case with trichloroethane (TCE) spills. Actually, zones of high NAPL content may even be undetected in case of local equilibrium, since high retardation involves long arrival times and extensive spreading and dilution of the effluent breakthrough curves. Payne et al. (1998) showed, through computer simulations, that inaccuracies in concentration determinations may have important detrimental effects on partitioning tracer tests performed in heterogeneous aquifers. We thus extend their argument to include heterogeneous NAPL distributions and their concomitant effect on water permeability and exchange of partitioning tracers between the aqueous and non-aqueous phase.

To broadly assess how close our system was to equilibrium conditions, we make use of the results of the inverse procedure at the sampling ports. Although, we already stated that ω values determined by the fitting procedure should be interpreted with caution, they, a priori, apply to sites presenting an intermediate level of non-equilibrium, i.e. they fall between sites attaining instantaneous equilibrium ($\omega \rightarrow \infty$) and those that remain undetected ($\omega \rightarrow 0$). Consequently, these values might be a coarse indicator of the rate at which partitioning tracer exchange took place in our aquifer model. Following Valocchi (1985), we make use of the deviation in the second central moment between measured and hypothetical equilibrium effluent breakthrough curves as an index of non-equilibrium behavior. The non-dimensional number obtained by Valocchi (1985) takes the following form in our case of a two-site partitioning model:

$$\varepsilon_2 = \frac{P}{\omega}(1-\beta)^2 = \frac{v^2}{\alpha D}\frac{(1-\beta)}{R} \tag{17}$$

Valocchi (1985) showed that low values for ε_2 correspond to conditions close to equilibrium exchange. As we typically obtained 500 as a value for ε_2, calculated from the results of the inverse procedure at the sampling ports (Tables 2 and 3), it strongly suggests that the tracer partitioning at numerous DNAPL occurrences in our flow container was taking place under non-equilibrium conditions. However, it is unclear if any tail extrapolation technique, applied to the extraction well samples, would have been able to really take undetected NAPL into account. It is expected that the data used during fitting of the tailing part of a breakthrough curve by an extrapolating function is generally unlikely to represent the contributions from high retardation and slow transfer areas, which might reach the extraction location at much larger times only. This behavior is illustrated in our study, since the inverse procedure performed on the sampling port data can be considered to encompass an extrapolation scheme, and it did not result in strikingly better DNAPL estimates than the non-extrapolated moment method.

A further investigation of the effects of porous medium and NAPL distribution heterogeneities on partitioning tracer exchanged should be performed with a computer model simulating tracer transport through zones containing different NAPL contents and tracer exchange rates. The model should also be used to analyze simulated breakthrough curves assuming concentration uncertainty, as suggested by Payne et al. (1998). The simultaneous effects of rate-limited tracer absorption, NAPL heterogeneity, porous medium heterogeneity, and tracer decay, on the partitioning tracer technique could also be assessed in light of concentration uncertainty. However, this kind of research is beyond the scope of this study.

4. Conclusion

A partitioning tracer test performed in a nominally two-dimensional, intermediate-scale aquifer model containing a tetrachloroethene (PCE) spill underestimated the amount of residual DNAPL and was insensitive to the presence of a pool comprising 30% of the contaminant. This was attributed to the low aqueous phase permeability within the DNAPL pool in combination with rate-limited partitioning of the tracers into the DNAPL. Our analysis indicate a general difficulty for the tracer technique to detect NAPL located in pools or large lenses.

Acknowledgements

This research was carried out as part of the US Environmental Protection Agency project R825409 "Investigation of the entrapment and surfactant enhanced recovery of NAPLs in heterogeneous sandy media". We would like to thank Dr Mart Oostrom of PNNL, Richland, WA, for his valuable comments during the review process, and Dr Cor Hofstee (TNO, Utrecht, The Netherlands) for his contribution to the experimental part of this study.

The two junior authors would like to express their sorrow about the untimely death of the senior author, Dr Marc Jalbert, of Lolier, France. At the time this manuscript was prepared, Marc was still a PhD student. We will remember him as a caring person and an outstanding scientist.

References

Annable, M.D., Rao, P.S.C., Hatfield, K., Graham, W.D., Wood, A.L., Enfield, C.G., 1998. Partitioning tracers for measuring residual NAPL: field scale test results. J. Environ. Engng 124, 497–502.

Augustijn, D.C.M., Gerstl, Z., Rao, P.S.C., 1991. Effects of sorbent matrix on sorption nonequilibrium of organic compounds. Proc. Am. Chem. Soc. Natl Meetings, Am. Chem. Soc. 31, 470–472.

Bear, J., 1972. Dynamics of fluids in porous media, Elsevier, New York.

Brusseau, M.L., 1992. Rate-limited mass transfer and transport of organic solutes in porous media that contain immobile immiscible organic liquid. Water Resour. Res. 28, 33–45.

Cameron, D.R., Klute, A., 1977. Convective–dispersive solute transport with a combined equilibrium and kinetic adsorption model. Water Resour. Res. 13, 183–188.

Coats, K.H., Smith, B.D., 1964. Dead-end pore volume and dispersion in porous media. Soc. Petrol. Engng 4, 73–84.

Cooke, C.E., Jr., 1971. Method of determining residual oil saturation. US Patent 3,590,923, US Patent Office, Washington, DC.

Cussler, E.L., 1984. Diffusion: Mass Transfer in Fluid Systems, Cambridge University Press, New York, NY.

Dane, J.H., Jalbert, M., Bahaminyakamwe, L., 1999. Investigation of the entrapment and surfactant enhanced recovery on nonaqueous phase liquids in heterogeneous sandy media. Vol. 2a. IV. PCE spill into a saturated, layered porous medium. V. Partitioning tracer experiments at the intermediate scale. VI. A non-equilibrium partitioning tracer inverse method to estimate residual NAPL. Department of Agronomy and Soils Special Report, Auburn University, AL, 170 p.

van Genuchten, M.Th., Wagenet, R.J., 1989. Two-site/two-region models for pesticide transport and degradation: theoretical development and analytical solutions. Soil Sci. Soc. Am. J. 53, 1303–1310.

van Genuchten, M.Th., Wierenga, P., 1976. Mass transfer studies in sorbing porous media. I. Analytical solutions. Soil Sci. Soc. Am. J. 40, 473–480.

Harvey, C.F., Gorelick, S.M., 1995. Temporal moment-generating equations: modeling transport and mass transfer in heterogeneous aquifers. Water Resour. Res. 31, 1895–1911.

Hatfield, K., Ziegler, J., Burris, D.R., 1993. Transport in porous media containing residual hydrocarbon. II. Experiments. J. Environ. Engng 199, 559–575.

Jackson, R.E., Pickens, J.F., 1994. Determining location and composition of liquid contaminants in geologic formations. US Patent 5,319,966. US Patent Office, Washington, DC.

James, A.I., Graham, W.D., Hatfield, K., Rao, P.S.C., Annable, M.D., 1997. Optimal estimation of residual non-aqueous phase liquid saturations using partitioning tracer concentration data. Water Resour. Res. 33, 2621–2636.

Jin, M., Delshad, M., Dwarakanath, V., McKinney, D.C., Pope, G.A., Sepehrnoori, K., Tilburg, C.E., Jackson, R.E., 1995. Partitioning tracer test for detection, estimation, and remediation performance assessment of subsurface nonaqueous phase liquids. Water Resour. Res. 31, 1201–1211.

Jury, W.A., Roth, K., 1990. Transfer Functions and Solute Movement through Soil: Theory and Applications, Birkhauser, Basel, Switzerland.

Lapidus, L., Amundson, N.R., 1952. Mathematics of adsorption in beds. VI. The effect of longitudinal diffusion in ion exchange and chromatographic columns. J. Phys. Chem. 56, 984–988.

Leij, F.J., Dane, J.H., 1991. Solute transport in a two-layer medium investigated with time moments. Soil Sci. Soc. Am. J. 55, 1529–1535.

Leij, F.J., Toride, N., 1998. Analytical solutions for nonequilibrium transport models. In: Selim, H.G., Ma, L. (Eds.), Physical Nonequilibrium in Soils, Modeling and Application, Ann Arbor Press, Chelsea, MI.

Nelson, N.T., Oostrom, M., Wietsma, T.W., Brusseau, M.L., 1999. Partitioning tracer method for the in situ measurement of DNAPL saturation: influence of heterogeneity and sampling method. Environ. Sci. Technol. 33, 4046–4053.

Nkeddi-Kizza, P., Biggar, J.W., Selim, H.M., van Genuchten, M.Th., Wierenga, P.J., Davidson, J.M., Nielsen, D.R., 1984. On the equivalence of two conceptual models for describing ion exchange during transport through an aggregated Oxisol. Water Resour. Res. 20, 1123–1130.

Oostrom, M., Hofstee, C., Dane, J.H., Lenhard, R.J., 1998. Single-source gamma radiation procedures for improved calibration and measurements in porous media. Soil Sci. 163, 646–656.

Oostrom, M., Hofstee, C., Walker, R.C., Dane, J.H., 1999. Movement and remediation of trichloroethylene in a saturated heterogeneous porous medium. 1. Spill behavior and initial dissolution. J. Cont. Hydrol. 37, 159–178.

Parker, J.C., van Genuchten, M.Th., 1984. Determining transport parameters from laboratory and field tracer experiments. Bull. 84-3, Va. Agric. Exp. St., Blacksburg, VA.

Passioura, J.B., 1971. Hydrodynamic dispersion in aggregated media. 1. Theory. Soil Sci. 111, 339–344.

Payne, T., Brannan, J., Falta, R., Rossabi, J., 1998. Detection limit effects on interpretation of NAPL partitioning tracer tests. In: Wickramanayake, G.B., Hinchee, R.E. (Eds.), Non-aqueous Phase Liquids, Remediation of Chlorinated and Recalcitrant Compounds, Battelle Press, Columbus, OH.

Sardin, M., Schweich, D., Leij, F.J., van Genuchten, M.Th., 1991. Modeling the sorption of linearly interacting solutes in porous media: a review. Water Resour. Res. 27, 2287–2307.

Selim, H.M., Davidson, J.M., Mansell, R.S., 1976. Evaluation of a two-site adsorption–desorption model for describing solute transport in soil. Proc. Comp. Simul. Conf., Am. Inst. Chem. Engng, New York, 444–448.

Tang, J.S., 1992. Interwell tracer test to determine residual oil saturation to waterflood at Judy Creek BHL A pool. J. Can. Pet. Tech. 31, 61.

Toride, N., Leij, F.J., van Genuchten, M.Th., 1995. The CXTFIT Code for Estimating Transport Parameters from Laboratory or Field Tracer Experiments, Version 2.0, US Salinity Laboratory, USDA, Riverside, CA.

Valocchi, A.J., 1985. Validity of the local equilibrium assumption for modeling sorbing solute transport through homogeneous soils. Water Resour. Res. 21, 808–820.

Wang, P., Dwarakanath, V., Rouse, B.A., Pope, G.A., Sepehmoori, K., 1998. Partition coefficients for alcohol tracers between nonaqueous-phase liquids and water from UNIFAC-solubility method. Adv. Water Resour. 21, 171–181.

Wise, W.R., Dai, D., Fitzpatrick, E.A., Evans, L.W., Rao, P.S.C., Annable, M.D., 1999. Non-aqueous phase characterization via partitioning tracer tests: a modified Langmuir relation to describe partitioning nonlinearities. J. Contam. Hydrol. 36, 153–165.